Long-period, longitudinal spin density modulation in an itinerant 5f magnetic compound UCu_2Si_2

2006 J. Phys.: Condens. Matter 18 479

(http://iopscience.iop.org/0953-8984/18/2/010)

INSTITUTE OF PHYSICS PUBLISHING JOURNAL OF PHYSICS: CONDENSED MATTER

J. Phys.: Condens. Matter **18** (2006) 479–492 doi:10.1088/0953-8984/18/2/010

Long-period, longitudinal spin density modulation in an itinerant 5f magnetic compound UCu_2Si_2

F Honda[1], **N Metoki**[1,2], **T D Matsuda**[1], **Y Haga**[1] **and Y Ōnuki**[1,3]

[1] Advanced Science Research Center, JAERI, Tokai, Ibaraki 319-1195, Japan
[2] Department of Physics, Tohoku University, Sendai 980-8578, Japan
[3] Graduate School of Science, Osaka University, Toyonaka, Osaka 560-0043, Japan

E-mail: honda.fuminori@jaea.go.jp

Received 16 June 2005, in final form 7 October 2005
Published 14 December 2005
Online at stacks.iop.org/JPhysCM/18/479

Abstract

The magnetic structure of UCu_2Si_2 has been studied by means of neutron scattering. We have observed the first- and very weak third-order incommensurate satellite reflections for 100 K $< T <$ 106 K with the propagation $\mathbf{q} = [0\,0\,\delta]$, $\delta = 0.116$ at $T = 101$ K, indicating nearly sinusoidal magnetic modulation with long periodicity of $\Lambda = 85.7$ Å. The intensity of the first-order satellite reflections is consistent with a moment direction parallel to the c-axis. The second-order satellite due to lattice modulation accompanied by a charge density wave could not be detected within our experimental sensitivity. The long-period magnetic modulation in UCu_2Si_2 cannot be explained in terms of an ANNNI model based on frustrated antiferromagnetic short-range interactions. The nearly sinusoidal long-period modulation is evidence for a spin density wave state as a consequence of itinerant behaviour of the 5f electrons in UCu_2Si_2. The ferromagnetic ground state and the very weak upper critical field for the incommensurate phase are consistent with the long periodicity.

(Some figures in this article are in colour only in the electronic version)

1. Introduction

The wide variety of f-electron compounds provides ample opportunity for systematic studies of electronic properties from both the fundamental interest and application points of view. This variety is a consequence of the many different kinds of f-electron states with multipolar degrees-of-freedom, such as charge, magnetic dipole, and quadrupole. Furthermore, the f electrons play an important role in the heavy-fermion character, and in valence fluctuations, multipolar ordering, and unconventional superconductivity in the vicinity of quantum critical points. For a systematic understanding of the nature of f electrons, it is very important to study families of compounds with the same crystal structure composed of a series of 4f rare-earth and 5f

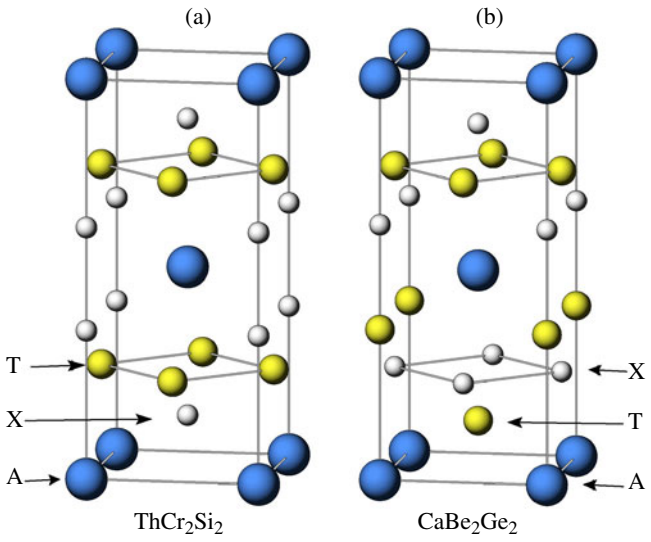

Figure 1. A schematic view of the crystal structure of (a) $ThCr_2Si_2$-type and (b) $CaBe_2Ge_2$-type structure of AT_2X_2 compounds, respectively. The large, middle, and small spheres represent the position of the rare-earth or actinide element A, transition metal T, and X = Si or Ge atom, respectively.

actinide elements having different f electron numbers and character, and with ligand elements having a variety of s, p, and d electrons hybridized with the f electrons. The AT_2X_2 family of f-electron compounds (A: rare-earth and actinide elements, T: transition metals, and X: Si or Ge) is a well known system, which has many members based on rare-earth [1] and actinide elements (Th, U, Np, Pu) [2]. Very high-quality single-crystal samples are also available for some of them. The crystal structures of $ThCr_2Si_2$-type (space-group $I4/mmm$) or $CaBe_2Ge_2$-type (space group $P4/nmm$) systems are very simple, as shown in figure 1. The electronic structure can be controlled with transition metal elements, which have different numbers of d electrons with various valence and conduction electron levels and bandwidths. The f–d hybridization is controlled via the lattice parameter, which is slightly different for Si and Ge compounds, and can be tuned by forming solid solutions, or by applying pressure or an external field. Consequently, a wide variety of interesting and unusual electronic properties has been reported for these systems. Some examples are itinerant and localized magnetic order, hidden order, heavy Fermion or non-Fermi liquid behaviour, and unconventional superconductivity.

In the present study we have focused on the U-based compound UCu_2Si_2. The crystal structure of this compound is $ThCr_2Si_2$-type, as shown in figure 1(a). In this structure, the U atoms are on the body-centred tetragonal sites. The magnetic structure and the phase diagram of UCu_2Si_2 were controversial and mysterious for a long time [3–8]. Both the existence and the absence of an antiferromagnetic phase occurring between the paramagnetic and ferromagnetic phases have been reported. The magnetic structure of such an antiferromagnetic phase remains unknown. There are also conflicting discussions about the occurrence of a first-order transition from the ferromagnetic to the antiferromagnetic state at 50 K [4–6]. The magnetic moment of uranium, $\simeq 1.75\ \mu_B$/U [8], in the ferromagnetic ground state is relatively high among uranium-based intermetallic compounds. A simple ferromagnetic ground state is rarely found in UT_2X_2, although a ferromagnetic ground state has been reported in Np- and Pu-based compounds [9–12]. A ferrimagnetic structure with finite spontaneous magnetization has been reported in UNi_2Si_2 [13].

Very recently, a high-quality single-crystal sample of UCu_2Si_2 has been grown by means of the Sn-flux method, and the macroscopic properties have been systematically measured [8]. The $ThCr_2Si_2$-type crystal structure was confirmed by means of single-crystal x-ray diffraction experiments. The lattice parameters obtained are $a = 3.981$ and $c = 9.943$ Å at room temperature. The magnetic phase diagram has been determined by means of electrical resistivity, specific heat, and magnetization measurements. The existence of an antiferromagnetic phase has been confirmed in a narrow temperature range between the Néel temperature $T_N = 106$ K and the ferromagnetic transition temperature $T_C = 100$ K, in a magnetic field less than 1.1 kOe along the c-axis. The ground state exhibits ferromagnetic order with a uranium magnetic moment of 1.75 μ_B/U, which is consistent with previous studies [3]. The transition between the antiferromagnetic and ferromagnetic states is of the first order, followed by a large and sharp-peaked specific heat anomaly at T_C. The magnetic susceptibility χ shows Curie–Weiss behaviour at high temperatures with an effective moment of 3 μ_B, which is slightly smaller than the theoretical effective moments of free U^{3+} or U^{4+} ions, and a positive Weiss temperature of 97 K along the c-axis, indicating dominant ferromagnetic interactions between uranium 5f moments. A strong uniaxial anisotropy was observed in the susceptibility measurement. The easy axis is parallel to the c-axis both in the paramagnetic and magnetically ordered states. The DC susceptibility, $\chi \parallel c$, abruptly decreases at $T = T_N$ as a result of the antiferromagnetic ordering, but recovers with further decreasing temperature, and increases significantly in the ferromagnetic state. The electrical resistivity in the basal plane is almost flat at high temperatures, but exhibits anomalies at T_C and T_N. The moderate electronic specific heat coefficient $\gamma = 20$ mJ mol^{-1} K^{-2} and the magnetically ordered moment smaller than the effective moment can be attributed to the itinerant character of the 5f electrons at low temperatures. In this paper, we report the results of our neutron scattering experiments on a single-crystal sample of UCu_2Si_2. We have found that an incommensurate longitudinal modulation of the uranium 5f moment is realized in the antiferromagnetic state. The long period ($\Lambda \simeq 85.7$ Å) of modulation, containing 17 ferromagnetic uranium sheets, as well as the small area of the antiferromagnetic phase in the magnetic phase diagram, indicates a dominant role for ferromagnetic interactions in the magnetic ordering. The long incommensurate modulation period cannot be reproduced in terms of an ANNNI (axial next-nearest-neighbour Ising) model based on frustrated, short-range antiferromagnetic interactions. On the other hand, this is strong evidence that an SDW (spin density wave) state occurs here as a consequence of the itinerant nature of the 5f electrons in this compound. From the similarity of the electronic and magnetic properties in other UT_2X_2 compounds, we speculate that the 5f electrons in these systems also have rather strong itinerant character.

2. Experimental procedure

Neutron scattering experiments were carried out on the cold and thermal neutron triple-axis spectrometers LTAS and TAS-2 installed in the guide hall of research reactor JRR-3 at the Japan Atomic Energy Research Institute (JAERI). Elastic scattering measurements were performed in the triple-axis mode. A neutron beam with energy $E = 5.0$ or 14.7 meV was monochromatized and analysed with vertically bent pyrolytic graphite (PG) monochromator and analyser crystals. Harmonic contamination was removed via a 20 cm thick Be polycrystalline block cooled down to 10 K and a PG filter as thick as 12 cm for cold and thermal neutron experiments, respectively. Collimators were not used, and thus the resolution ($\Delta q/q \simeq 0.02$) was determined by the beam divergence, the mosaic spread of the crystal, and by sample dimensions. The rocking curve full width at half maximum for fundamental reflections was typically $\simeq 0.4°$. Thus the sample

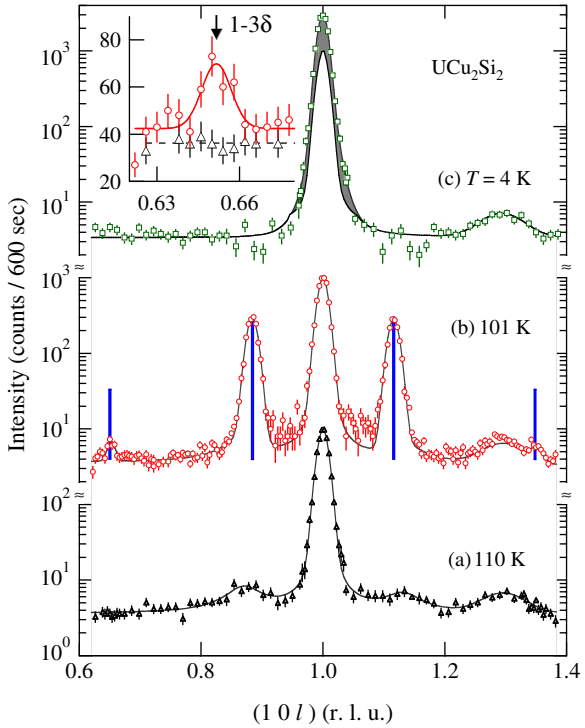

Figure 2. (1 0 l) scattering profiles for UCu_2Si_2 measured in the (a) paramagnetic phase at $T = 110$ K, (b) antiferromagnetic phase at $T = 101$ K, and (c) ferromagnetic phase at $T = 4$ K. The vertical scales are separated for clarity. The solid lines indicate the results of model calculations. The bars in (b) are the calculated intensities for the first- and third-order magnetic scattering, assuming square-wave modulation. The hatched area in (c) is the ferromagnetic scattering superposed on the nuclear peak measured in the paramagnetic phase. The magnified plot around the third-order satellite (1 0 1 − 3δ) is shown in the inset.

mosaic spread should be very small. The (h 0 l) scattering plane was scanned to determine the magnetic structure of UCu_2Si_2.

The single-crystal sample of UCu_2Si_2 was grown by the Sn-flux method. Details of the sample preparation technique and the macroscopic properties of single crystals of UCu_2Si_2 have been published elsewhere [8]. The dimensions of the single crystal used in the present neutron scattering experiment were 1 mm × 1 mm × 1 mm with total mass of 7 mg. The small residual resistivity $\rho_0^a = 2.3\ \mu\Omega$ cm and $\rho_0^c = 6.4\ \mu\Omega$ cm for $J \parallel [1\ 0\ 0]$ and $J \parallel [0\ 0\ 1]$, respectively, and the large residual resistivity ratio $\rho^a(300\ \mathrm{K})/\rho^a(4.2\ \mathrm{K}) \simeq 80$ indicate very high quality for our sample. In particular, ρ_0^c is much smaller than previously reported values for UT_2X_2 (T: Ni, Ru, Pd, Ir, Pt, etc), which is the signature for nearly perfect stacking without defects.

3. Results

Figure 2 shows the (1 0 l) scattering profile of UCu_2Si_2 measured in (a) the paramagnetic phase at $T = 110$ K, (b) the antiferromagnetic phase at $T = 101$ K, and (c) the ferromagnetic phase at $T = 4$ K. We have observed the first- and third-order satellite reflections at (1 0 1±δ) and (1 0 1±3δ), respectively, due to the incommensurate magnetic modulation in the

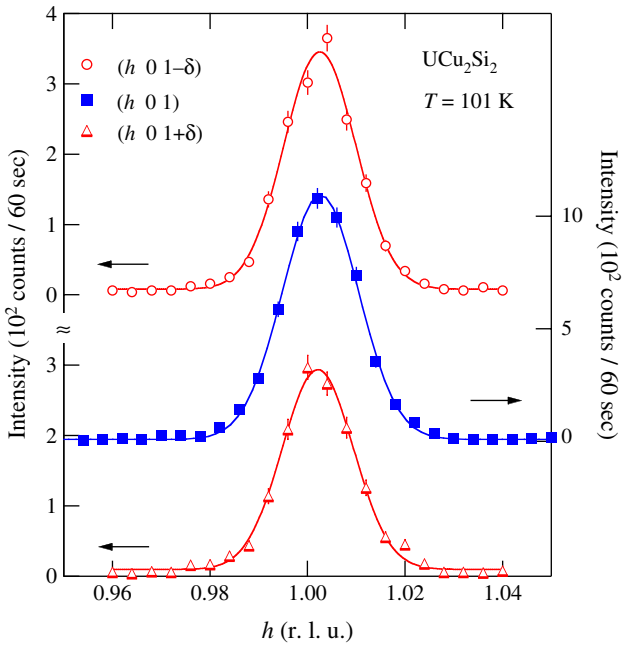

Figure 3. Scattering profiles of the $(h\ 0\ 1 \pm \delta)$, $\delta = 0.116$, incommensurate antiferromagnetic reflections and $(h\ 0\ 1)$ nuclear peak along the a^* =direction. The origins of the data are shifted for clarity.

antiferromagnetic phase. We obtained $\delta = 0.116$ at $T = 101$ K. No trace of the second-order satellite has been observed within our experimental accuracy. These incommensurate magnetic reflections disappear in the paramagnetic and ferromagnetic phases. At 110 K, a broad and weak scattering due to magnetic fluctuations is observed near the position of the first-order satellite peak. We observed a strong ferromagnetic scattering as indicated by the hatched area in figure 2(c), superposed on the (1 0 1) nuclear reflection. The estimated ferromagnetic moment is 2.0(1) μ_B/U, which is consistent with the magnetization measurements, 1.75 μ_B/U [8]. The broad feature around $l = 1.3$ is an unknown polycrystalline signal.

The scattering profile around the third-order satellite is shown in the inset of figure 2 on an expanded scale. We observed a very weak, but clear peak in the antiferromagnetic phase at $T = 101$ K, which, however, disappears in the paramagnetic phase at $T = 110$ K. The arrow indicates the expected position of a third-order satellite, $l = 1 - 3\delta = 0.652$ for $\delta = 0.116$ at $T = 101$ K. The peak position is in good agreement with this predicted position. The intensity of the third-order satellite, 25 counts/600 s, is less than 1% of the first-order satellite peak, $\simeq$3000 counts/600 s. This means that the modulation is almost sinusoidal, with very small third-order harmonics.

Figure 3 presents the results of the h-scan of the first-order satellite reflections at $(1\ 0\ 1 \pm \delta)$ and the (1 0 1) nuclear peak. We observed a clear incommensurate reflection peak centred at $h = 1$; hence, the propagation should be $[0\ 0\ \pm\delta]$ with $\delta = 0.116$ at $T = 101$ K. These results indicate that the magnetic structure is an incommensurate stacking of ferromagnetic basal planes with a long periodicity of $\Lambda \simeq 85.7$ Å along the c-axis.

The incommensurate satellite peaks in the antiferromagnetic phase of UCu_2Si_2 have been observed at positions symmetrical with respect to the fundamental reflections. Figure 4 shows representative data measured at $T = 101$ K. We found strong satellite peaks around the

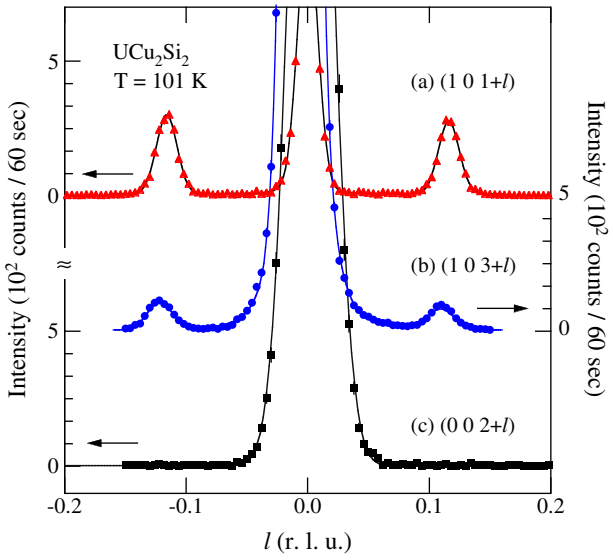

Figure 4. Scattering profiles of the incommensurate satellite peak around (a) (1 0 1), (b) (1 0 3), and (c) (0 0 2) fundamental reflections. The measured temperature is $T = 101$ K. The solid lines are the results of the model calculation based on longitudinal sinusoidal modulation along the c-axis with the periodicity $\Lambda = 85.7$ Å and the modulation amplitude $\simeq 1.3\ \mu_B$/U.

(a) (1 0 1) reflection, while the intensity is much weaker around the (b) (1 0 3) reflection. We observed no trace of the satellite peaks around the (c) (0 0 2) reflection, where the scattering vector Q is parallel to the c^*-axis. The absence of the magnetic satellite for $Q \parallel c$ indicates that the magnetic moment μ is parallel to the tetragonal c-axis. Furthermore, this moment direction $\mu \parallel c$ is consistent with the strong, uniaxial anisotropy observed for UCu_2Si_2 with the easy axis along the c-axis [8]. In order to confirm the direction of the magnetic moment, the integrated intensities of the first satellite peaks were measured and plotted in figure 5 as a function of $\sin^2\alpha$, where α is the angle between the scattering vector Q and the c^*-axis. The integrated intensity of the magnetic scattering for a non-polarized neutron beam is given as follows:

$$I_{\mathrm{mag}} = Ap^2|F_{\mathrm{M}}(Q)|^2 L(\theta)(\sin^2\alpha), \tag{1}$$

$$p = \frac{\gamma e^2}{2m_e c^2} = 0.2696 \times 10^{-12}\ (\mathrm{cm}), \tag{2}$$

where A, $L(\theta)$, $\sin\alpha$, and $F_{\mathrm{M}}(Q)$ are the scale factor, Lorenz factor, angle factor, and magnetic structure factor, respectively. As shown in figure 5, the normalized integrated intensity exhibits a linear relation with respect to $\sin^2\alpha$. Therefore, the direction of the magnetic moment is parallel to the c-axis.

Figure 6 shows the temperature dependence of the magnetic scattering intensities of the first- and third-order satellite observed at (1 0 0.883) and (1 0 0.65), respectively, and the ferromagnetic scattering at the (1 0 1) peak position obtained by subtracting the nuclear scattering intensity measured at $T = 110$ K. The inset shows a magnified plot around 100 K for clarity. Note that the data for the third-order satellite denoted by closed circles (•) are plotted with respect to the right-hand axis. The magnetic satellite peaks appear below $T < T_{\mathrm{N}} = 106$ K, and the intensity increases linearly with decreasing temperature. This continuous behaviour is consistent with that of a magnetic order parameter for a second-order

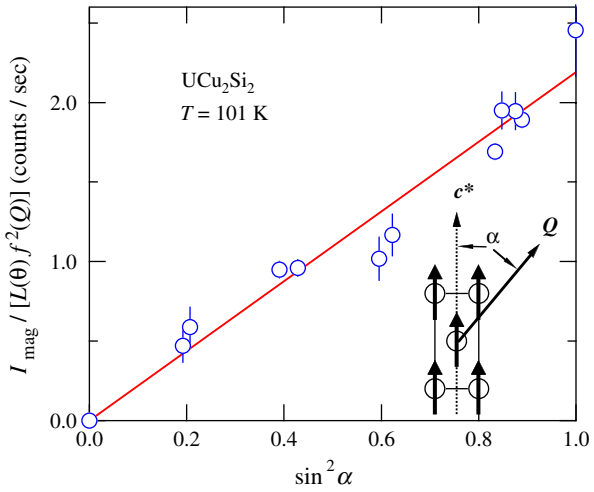

Figure 5. A plot of the normalized integrated intensities of the first satellite as a function of $\sin^2\alpha$, where α is the angle between the scattering vector **Q** and the c^*-axis (see the schematic view shown in the inset). The integrated intensity was normalized with the Lorentz factor and the magnetic form factor of the U^{3+} free ion. The straight line indicates a calculated result for the moment direction and the propagation parallel to the c-axis, where we assumed the periodicity $\Lambda = 85.7$ Å and an amplitude for the fundamental modulation as large as 1.3 μ_B/U.

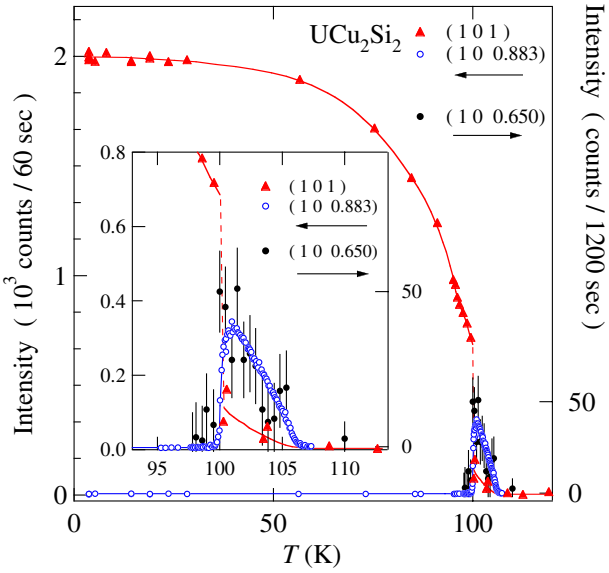

Figure 6. The first and third satellite intensities measured at (1 0 0.883) and (1 0 0.650) and the ferromagnetic scattering intensity at (1 0 1) reflection are plotted versus temperature. The closed triangles, open circles and closed circles indicate the data for (1 0 1), (1 0 0.883) and (1 0 0.650), respectively.

transition. Incommensurate satellite peaks were observed within a very narrow temperature region $T_C = 100$ K $< T < T_N$, where the antiferromagnetic phase is stable. With further decreasing temperature, the incommensurate satellite peaks disappear and there is a switch

to ferromagnetic scattering at T_C. The nearly discontinuous change of the reflection intensity indicates a first-order transition at $T = T_C$. This first-order behaviour is consistent with a sharp specific-heat peak and a discontinuous resistivity anomaly at $T = T_C$ [8]. The ferromagnetic intensity also increases linearly with decreasing temperature around T_C. The magnetic structure factor of a collinear system is given by

$$F_M(Q) = \sum_j \mu_j f_j(Q) \exp(i\mathbf{Q} \cdot \mathbf{r}_j), \tag{3}$$

where $f_j(Q)$ is the magnetic form factor, and μ_j is the magnetic moment for the jth site sitting at position $\mathbf{r}_j$. The magnetic moments in a one-dimensionally modulated structure can be expressed as

$$\mu_j = \sum_m \mu_m \cos(m\mathbf{q} \cdot \mathbf{r}_j) \qquad (m = \text{odd integer}), \tag{4}$$

where μ_m and $\mathbf{q}$ are the mth-order modulation amplitude and modulation vector, respectively. By substituting equation (4) into (3) we get the magnetic structure factor as follows:

$$F_M(Q) = f(Q) \sum_j \sum_m \frac{\mu_m}{2} [\exp[i\mathbf{r}_j \cdot (\mathbf{Q} + m\mathbf{q})] + \exp[-i\mathbf{r}_j \cdot (\mathbf{Q} - m\mathbf{q})]]. \tag{5}$$

Therefore, we should observe magnetic satellites at $\mathbf{Q} = \mathbf{Q}_0 \pm m\mathbf{q}$, where $\mathbf{Q}_0$ is the wavevector of the fundamental reflection. Using equation (5), we can calculate the intensities of magnetic reflections. The solid line in figure 2(b) is the result of such a model calculation with the periodicity $\Lambda = 85.7$ Å ($\mathbf{q} = [0\,0\,\delta]$, $\delta = 0.116$) and a modulation amplitude $\mu_1 = 1.3\ \mu_B$/U and $\mu_3 = 0.1\ \mu_B$/U for the first and third Fourier component, respectively. The line around $l = 1.3$ is taken to be an impurity peak. It should be noted that the experimental result is well reproduced by the model calculation. From our analysis, we have found that the first and third satellite peaks are resolution limited. On the other hand, the bars are the calculated magnetic intensity for square-wave modulation. The modulation amplitude is assumed to be 0.79 μ_B, which has a first-order Fourier component $\mu_1 = 1.3\ \mu_B$/U. In the case of the square-wave magnetic modulation, a remarkable third-order satellite as large as 10% of the first-order one should be observed. The observed intensity for the third-order satellite, which is less than 1% of the first-order satellite, is one order of magnitude smaller than that for the case of square-wave modulation. This means that the modulation of the antiferromagnetic structure in UCu_2Si_2 is almost sinusoidal. The calculated intensity assuming a modulation amplitude $\mu_1 = 1.3\ \mu_B$/U is shown as a solid line in figure 6. This calculated intensity is in good agreement with experimental results. It should be noted that the root-mean-square average of the modulation amplitude,

$$\sqrt{\overline{(\mu_1)^2}} = 0.9\ \mu_B/\text{U}, \tag{6}$$

is very close to the ferromagnetic moment $\simeq 0.8\ \mu_B$/U at $T = T_C$ obtained in the present neutron scattering experiments and the magnetization measurements [8]. The observed and calculated integrated intensities of the first-order, incommensurate satellite peaks in the AF phase are summarized in table 1. The experimental results agree well with the model calculation, assuming a modulation amplitude 1.3(1) μ_B/U for the first-order Fourier component along the c-axis and the propagation $\delta = 0.116$.

The magnetic structures for UCu_2Si_2 determined with the present neutron scattering experiments are shown schematically in figure 7. A simple ferromagnetic ordering as shown in figure 7(a) is stable in the ground state and, most likely, in a metamagnetic phase with magnetic field applied along the c-axis. In a very small region for $T_C < T < T_N$ and $H \leqslant 1$ kOe, an incommensurate (antiferromagnetic) structure with longitudinal spin density

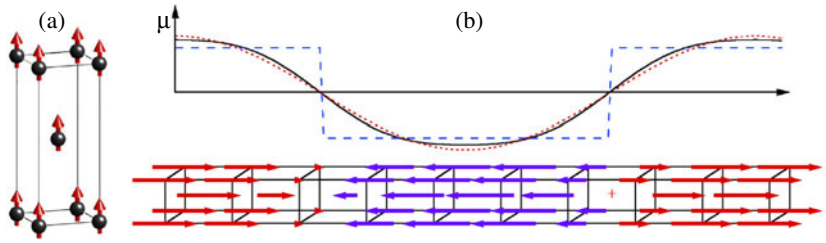

Figure 7. Derived magnetic structures for (a) the ground-state simple ferromagnetic ordering and (b) the incommensurate longitudinal antiferromagnetic structure for 100 K $< T <$ 106 K. The solid, dotted and dashed lines indicate the experimentally determined modulation of the magnetic moment for UCu_2Si_2, and calculated moment modulation for sinusoidal and square wave modulation, respectively.

Table 1. The observed and calculated magnetic scattering intensities.

		AFM ($T = 101$ K)		FM ($T = 10$ K)	
Index	$l \pm \delta$	I_{obs}	I_{cal}	I_{obs}	I_{cal}
(1 0 1)	−	2.61 ± 0.07	2.60	22.9 ± 0.4	22.7
	+	2.24 ± 0.07	2.34		
(1 0 3)	−	0.79 ± 0.05	0.75	3.0 ± 1.5	6.4
	+	0.73 ± 0.04	0.64		
(1 0 5)	−	0.26 ± 0.06	0.19	4.4 ± 1.3	1.6
	+	0.19 ± 0.04	0.17		
(2 0 0)	−	1.28 ± 0.15	1.11	12.0 ± 2.0	10.2
	+	1.28 ± 0.15	1.11		
(2 0 2)	−	0.89 ± 0.06	0.86	6.2 ± 0.7	8.7
	+	0.87 ± 0.05	0.80		
(2 0 4)	−	0.38 ± 0.04	0.43	4.8 ± 1.5	3.8
	+	0.32 ± 0.04	0.40		
(0 0 2)	±	0.0	0.0	0.0	0.0

modulation appears (figure 7(b)). The envelope of the moment amplitude is indicated by the solid curve in figure 7(b). This curve is very close to the sinusoidal modulation shown as a dotted line, but quite different from the square-wave modulation drawn as a dashed line. The long periodicity $\Lambda = 85.7$ Å corresponds to roughly 17 uranium basal planes. Therefore, there is a large ferromagnetic region in each half period consisting of more than eight layers. The existence of the large ferromagnetic region is consistent with the small critical field for the incommensurate phase.

Figure 8 shows the temperature dependence of the incommensurate satellite peaks scanned along the c^*-direction. We have found that the satellite peaks shift slightly towards the fundamental peak position (1 0 1) with decreasing temperature. This means that the periodicity Λ increases slightly, where $\Lambda \rightarrow \infty$ corresponds to the ferromagnetic structure. Therefore, this shift is considered to be a weak precursor of the first-order ferromagnetic transition at T_C. The temperature dependence of the modulation δ and the periodicity Λ are plotted in figure 9.

The modulation amplitude of the first-order satellite μ_1 is plotted with respect to the temperature in figure 10. The temperature dependence of the ferromagnetic moment μ is also indicated. With decreasing temperature, a remarkable increase of the modulation amplitudes in the incommensurate phase is revealed by our neutron scattering experiment. It should be noted that the modulation amplitude at 101 K is comparable to the ferromagnetic moment

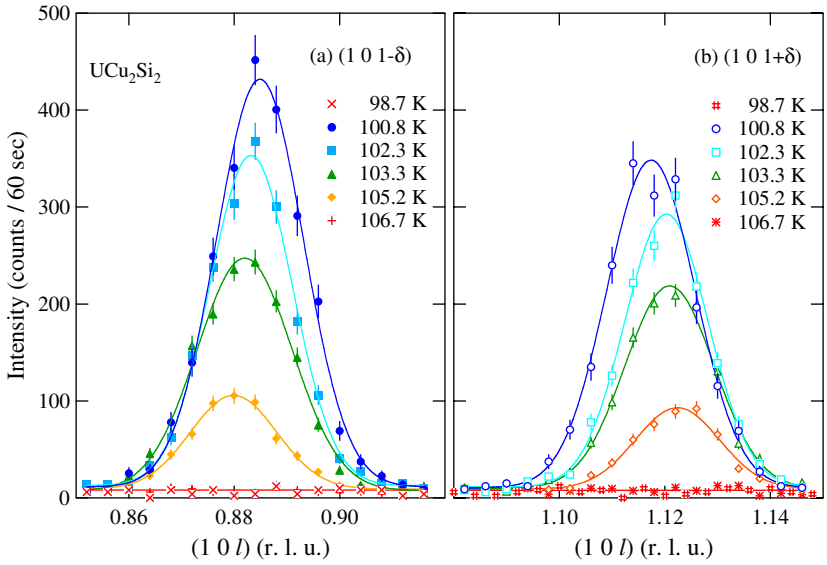

Figure 8. The temperature dependence of the (a) (1 0 1−δ) and (b) (1 0 1+δ) scattering peak profiles along the l-direction, shown for the series of temperatures indicated.

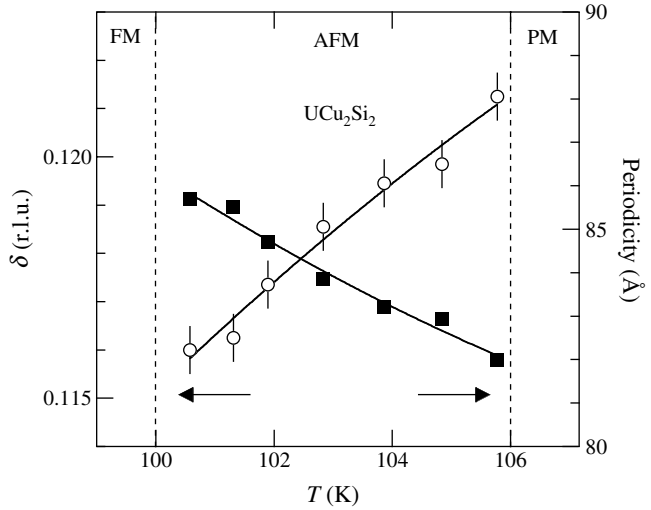

Figure 9. The temperature dependence of the incommensurate modulation δ and the periodicity Λ, denoted by open circles and closed squares, respectively.

at T_C ($\simeq$0.8 μ_B/U). The scattering intensity of the first satellite reflection increases linearly with decreasing temperature, as shown in figure 6. This means that the amplitude would be proportional to $T^{1/2}$. This mean-field-like behaviour reminds us of an SDW state with developing gap formation. Thus, a BCS-like temperature dependence of the magnetic order parameter is expected, which is consistent with the mean-field behaviour near the transition temperature. The solid line in figure 10 is the temperature dependence of the order parameter in weak-coupling BCS theory. For $T \approx T_c$, the order parameter Δ can be expressed as

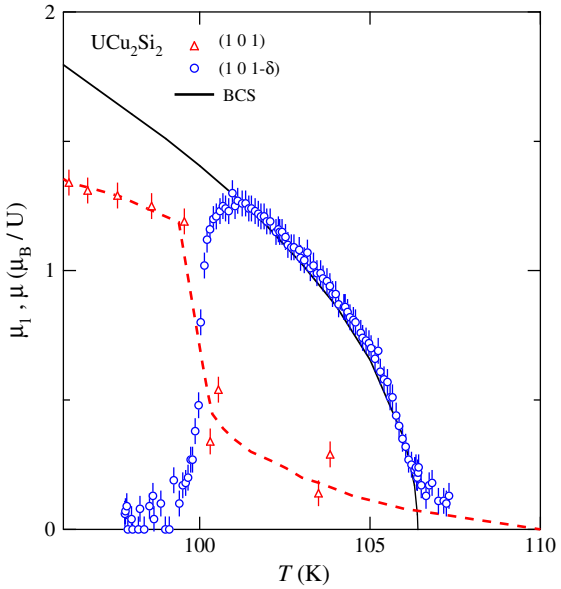

Figure 10. The temperature dependence of the amplitude μ_1 (open circles) of the first-order magnetic modulation in UCu_2Si_2. The size of the measured uniform ferromagnetic moment μ (open triangles) is also plotted as a function of temperature. The solid line denotes the temperature dependence of the order parameter derived from weak-coupling BCS theory for $T \simeq T_c$.

$$\frac{\Delta(T)}{\Delta(0)} \approx 1.74\left[\left(1-\frac{T}{T_c}\right)\right]^{1/2}. \tag{7}$$

This calculated curve is consistent with the experimental data near T_N.

The integrated intensities of the ferromagnetic scattering at 10 K have been obtained by subtracting the nuclear scattering intensities measured at 110 K. The obtained integrated intensities and calculated results assuming a ferromagnetic moment of 2.0(1) μ_B/U along the c-axis are also shown in table 1. The slightly larger moment value compared to the magnetization measurements [8] could be due to experimental error caused by the large nuclear background and/or slight changes of the magnetic form factor for uranium in UCu_2Si_2 relative to that of the free U^{3+} ion. In order to confirm this, more precise measurements of the magnetic form factor using polarized neutrons are in progress.

4. Discussion

The most remarkable result of this neutron scattering study on UCu_2Si_2 is the unusual magnetic structure showing an incommensurate longitudinal modulation. The small propagation vector $\mathbf{q} = [0\,0 \pm 0.116]$ corresponds to a very long periodicity $\Lambda \simeq 85.7$ Å. In comparison with the lattice constant $c = 9.943$ Å, 17 layers of ferromagnetically ordered basal planes are involved in a modulation period as shown in figure 8. This long-period modulation is strong evidence for an SDW (spin density wave) state in UCu_2Si_2. Furthermore, the temperature dependence of the modulation amplitude is in good agreement with a BCS-type temperature dependence as shown by the solid line in figure 12. Thus, the 5f electrons in this compound have strong itinerant character.

Figure 11 shows the temperature dependence of the electrical resistivity ρ^a taken from [8] and ρ^c for the current along the [1 0 0] and [0 0 1] directions. The electrical resistivity

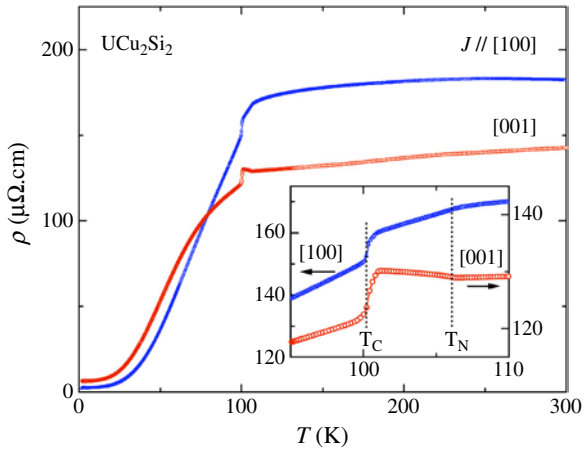

Figure 11. The temperature dependence of the electrical resistivity of UCu_2Si_2 for current parallel and perpendicular to the *c*-axis shown by circles and triangles, respectively.

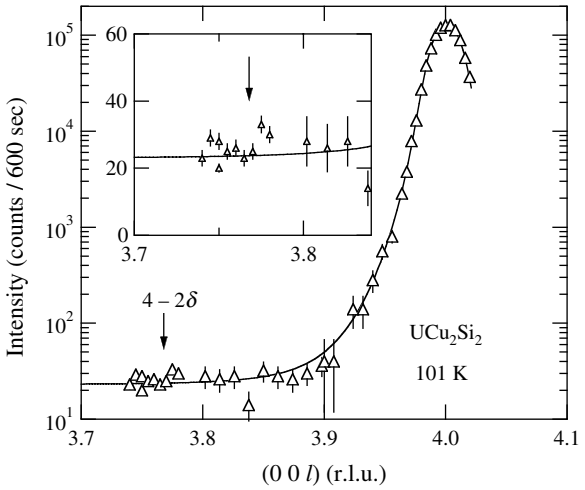

Figure 12. The line scan over the first and second satellite reflections of the (0 0 4) peak measured at 101 K.

was measured by means of a standard four-probe method. The resistivity shows very weak temperature dependence down to T_N, while remarkably anisotropic behaviours have been observed below T_N. In particular, ρ^c increases and ρ^a decreases with decreasing temperature in this region. The increase of the resistivity ρ^c is consistent with a gap opening in the SDW/CDW state with the modulation $\mathbf{q} = [0\ 0\ \delta]$. The upturn in ρ^c at T_N is characteristic of SDW/CDW transitions and has often been observed in many UT_2X_2 compounds [14–16]. For example, ρ^c in UNi_2Ge_2 exhibits a huge hump reflecting the gap opening at T_N [15]. We could not estimate the gap energy from the resistivity data because of the first-order transition from the SDW/CDW state to the FM ground state. Both ρ^a and ρ^c show a discontinuous decrease at T_C. In the FM state, ρ^a decreases linearly with decreasing temperature, while ρ^c has a shoulder around 75 K. The residual resistivities along both axes are quite small: $\rho_0^a = 2.3\ \mu\Omega$ cm and $\rho_0^c = 6.4\ \mu\Omega$ cm, respectively.

In previous studies the same type of longitudinal modulated structure has been reported in, for example, UNi_2Si_2 [3] and UPd_2Si_2 [17]. However, the periodicity $\Lambda = 37$ Å for both compounds is much shorter than for UCu_2Si_2 ($\Lambda = 85.7$ Å). The magnetic structure and phase diagram of UPd_2Si_2 and UNi_2Si_2 have been analysed in terms of the ANNNI model [16, 18] and an extension of the ANNNI model [19, 20], respectively. This interpretation is based on a localized picture of the 5f electrons. We argue that the ANNNI model cannot be relevant to the long-period modulation found in UCu_2Si_2. In this model, frustration between competing antiferromagnetic interactions up to the second-nearest neighbour is essential. Therefore the magnetic structures derived in the ANNNI model are described with sequences of polarities, i.e., '$+-+$' or '$++-$', which represent discrete sets of infinite numbers of structures with long periodicity, called the devil's staircase [21, 22]. Long periodicity in a system with short-range and frustrated interactions is an essential point in the ANNNI model. However, this is not the case for UCu_2Si_2. The long-period incommensurate modulation realized in UCu_2Si_2 does not belong to this category. In this structure, there is a long ferromagnetic sequence consisting of eight basal planes in a half period, as shown in figure 7. Such a long-period ferromagnetic sequence cannot be reproduced based on an ANNNI model.

The physical properties of UCu_2Si_2, UNi_2Si_2, and also UPd_2Si_2, are very similar. They have the same crystal structure with almost identical structural parameters, and the electronic structure should also be very similar. Therefore it is quite reasonable to consider that the 5f electrons in these compounds have strong itinerant character. Actually, several UT_2X_2 compounds exhibit resistivity anomalies characteristic of the SDW state around the magnetic ordering temperatures [14–16]. Such anomalies are reminiscent of the SDW antiferromagnet chromium around $T_N \simeq 312$ K [23–25]. Thus, we conclude that the strong itinerant character of 5f electrons is the most remarkable feature of the UT_2X_2 family.

The mechanism for spin density wave formation is the lowering of the energy of a conduction band which carries magnetism by forming a gap at a nesting vector. The difference in the electron density modulation for spin up and spin down creates an SDW state. Thus, a charge density wave (CDW) with a propagation vector of $2\mathbf{q}$, where $\mathbf{q}$ is the magnetic propagation vector, should be accompanied by an SDW state. Actually, in 3d electron systems, typically in Cr, the coexisting SDW and CDW have been observed by means of neutrons as well as with x-rays, which is the definitive experimental evidence for the SDW transition in Cr [26]. To the best of our knowledge, such a clear SDW/CDW state has not been reported so far in uranium intermetallic compounds. A clear CDW transition in α-uranium accompanies no magnetic ordering. One of the reasons for the lack of observations of typical SDW/CDW states is that few uranium intermetallic compounds exhibit incommensurate magnetic ordering, whereby the CDW peak at $2\mathbf{q}$ would occur at a different position from those of strong fundamental reflections.

Figure 12 shows the line scan around (0 0 4) at 101 K. Even in our very careful neutron scattering experiments, we could observe no trace of the second-order satellite at $(0\,0\,4-2\delta)$ within our statistical accuracy corresponding to 5×10^{-4} of the intensity of the (0 0 4) reflection, i.e., the strongest fundamental nuclear reflection. Therefore a CDW can be observed via nuclear cross section of the lattice modulation only if the modulation is large enough to detect. In this sense the resonant x-ray technique is the most suitable probe to establish the existence of a 5f-electron SDW/CDW state. A non-resonant x-ray study on UCu_2Si_2 is in progress.

5. Conclusion

In addition to the ferromagnetic ground state, an incommensurate SDW state with longitudinal and nearly sinusoidal modulation is revealed for a narrow temperature range (100–106 K) in

UCu_2Si_2. The long periodicity $\simeq$85.7 Å is the most remarkable feature for the itinerant SDW state. It implies a strong itinerant character for the 5f electrons in UT_2X_2 systems.

Acknowledgments

The authors would like to thank K Kaneko and S Jonen for fruitful discussion and technical support in neutron scattering experiments. The authors would like also to thank Professor R E Walstedt for critical reading and fruitful discussion of the manuscript. A part of this work is financially supported by the Grant-in-aid KAKENHI No 14340112, the Grant-in-Aid for Scientific Research (A), (C), Creative Scientific Research (15GS0213) from the Japan Society for the Promotion of Science and Scientific Research of Priority Area 'Skutterudite' (No 16037215) from the Ministry of Education, Science, Sports and Culture.

References

[1] See, for example Szytula A and Leciejewicz J 1989 *Handbook on the Physics and Chemistry of the Rare Earth* vol 12, ed K A Gschneidner Jr and L Eyring (Amsterdam: North-Holland) p 133
[2] Sechovsky V and Havela L 1998 *Handbook of Magnetic Materials* vol 11, ed K H J Bushow (Amsterdam: Elsevier Science B.V.) p 1 and references therein
[3] Chelmicki L, Leciejewicz J and Zygmunt A 1985 *J. Phys. Chem. Solids* **46** 529
[4] Kuznietz M, Andre G, Bouree F, Pinto H, Ettedgui H and Melamud M 1995 *J. Alloys Compounds* **219** 244
[5] Fisk Z, Moreno N O and Thompson J D 2003 *J. Phys.: Condens. Matter* **15** S1917
[6] Kuznietz M 2003 *J. Phys.: Condens. Matter* **15** 8957
[7] Fisk Z, Moreno N O, Thompson J D and Hundley M F 2003 *J. Phys.: Condens. Matter* **15** 8967
[8] Matsuda T D, Haga Y, Ikeda S, Galatanu A, Yamamoto E, Shishido H, Yamada M, Yamaura J, Hedo M, Uwatoko Y, Matsumoto T, Tada T, Noguchi S, Sugimoto T, Kuwahara K, Iwasa K, Kohgi M, Settai R and Onuki Y 2005 *J. Phys. Soc. Japan* **74** 1552
[9] Gal J, Koupp M, Hadari Z and Nowik I 1976 *Solid State Commun.* **20** 421
[10] de Novion C H, Gal J and Buevoz J L 1980 *J. Magn. Magn. Mater.* **21** 85
[11] Wastin F, Rebizant J, Spirlet J C, Sari C, Walker C T and Fuger J 1993 *J. Alloys Compounds* **196** 87
[12] Wastin F, Rebizant J, Spirlet J C, Fuger J, Kanellakopulos B and Sechovsky V 1993 *J. Alloys Compounds* **193** 119
[13] Lin H, Rebelsky L, Collins M F, Garrett J D and Buyers W J L 1991 *Phys. Rev.* B **43** 13232
[14] Palstra T T M, Menovsky A A, van den Berg J, Dirkmaat A J, Kes P H, Nieuwenhuys G J and Mydosh J A 1985 *Phys. Rev. Lett.* **55** 2727
[15] Ning Y B, Garrett J D, Stager C V and Datars W R 1992 *Phys. Rev.* B **46** 8201
[16] Honma T, Amitsuka H, Yasunami S, Tenya K, Sakakibara T, Mitamura H, Goto T, Kido G, Kawarazaki S, Miyako Y, Sugiyama K and Date M 1998 *J. Phys. Soc. Japan* **67** 1017
[17] Shemirani B, Lin H, Collins M F, Stager C V, Garett J D and Buyers W J L 1993 *Phys. Rev.* B **47** 8672
[18] Plumer M L 1994 *Phys. Rev.* B **50** 13003
[19] Mailhot A, Plumer M L, Caille A and Azaria P 1992 *Phys. Rev.* B **45** 10 399
[20] Muraoka Y 2001 *Phys. Rev.* B **64** 134416
[21] Selke W 1988 *Phys. Rep.* **170** 3466
[22] Bak P 1982 *Rep. Prog. Phys.* **45** 587
[23] Fawcett E 1988 *Rev. Mod. Phys.* **60** 209
[24] Miwa H 1963 *Prog. Theor. Phys.* **29** 477
[25] Suezaki Y and Mori H 1969 *Prog. Theor. Phys.* **41** 1177
[26] Tsunoda Y, Mori M, Kunitomi N, Teraoka Y and Kanamori J 1974 *Solid State Commun.* **14** 287